

**Precise measurement of $\mathcal{B}(\tau^- \rightarrow K^{*0}(892)K^- \nu_\tau)$ and
the mass and width of the $K^{*0}(892)$ meson**

I. Adachi,¹⁰ H. Aihara,⁵¹ D. Anipko,¹ K. Arinstein,¹ T. Aso,⁵⁵ V. Aulchenko,¹ T. Aushev,^{22,16}
T. Aziz,⁴⁷ S. Bahinipati,³ A. M. Bakich,⁴⁶ V. Balagura,¹⁶ Y. Ban,³⁸ E. Barberio,²⁵ A. Bay,²²
I. Bedny,¹ K. Belous,¹⁵ V. Bhardwaj,³⁷ U. Bitenc,¹⁷ S. Blyth,²⁹ A. Bondar,¹ A. Bozek,³¹
M. Bračko,^{24,17} J. Brodzicka,^{10,31} T. E. Browder,⁹ M.-C. Chang,⁴ P. Chang,³⁰ Y.-W. Chang,³⁰
Y. Chao,³⁰ A. Chen,²⁸ K.-F. Chen,³⁰ B. G. Cheon,⁸ C.-C. Chiang,³⁰ R. Chistov,¹⁶ I.-S. Cho,⁵⁷
S.-K. Choi,⁷ Y. Choi,⁴⁵ Y. K. Choi,⁴⁵ S. Cole,⁴⁶ J. Dalseno,¹⁰ M. Danilov,¹⁶ A. Das,⁴⁷
M. Dash,⁵⁶ A. Drutskoy,³ W. Dungel,¹⁴ S. Eidelman,¹ D. Epifanov,¹ S. Esen,³ S. Fratina,¹⁷
H. Fujii,¹⁰ M. Fujikawa,²⁷ N. Gabyshev,¹ A. Garmash,³⁹ P. Goldenzweig,³ B. Golob,^{23,17}
M. Grosse Perdekamp,^{12,40} H. Guler,⁹ H. Guo,⁴² H. Ha,¹⁹ J. Haba,¹⁰ K. Hara,²⁶ T. Hara,³⁶
Y. Hasegawa,⁴⁴ N. C. Hastings,⁵¹ K. Hayasaka,²⁶ H. Hayashii,²⁷ M. Hazumi,¹⁰ D. Heffernan,³⁶
T. Higuchi,¹⁰ H. Hödlmoser,⁹ T. Hokuue,²⁶ Y. Horii,⁵⁰ Y. Hoshi,⁴⁹ K. Hoshina,⁵⁴ W.-S. Hou,³⁰
Y. B. Hsiung,³⁰ H. J. Hyun,²¹ Y. Igarashi,¹⁰ T. Iijima,²⁶ K. Ikado,²⁶ K. Inami,²⁶ A. Ishikawa,⁴¹
H. Ishino,⁵² R. Itoh,¹⁰ M. Iwabuchi,⁶ M. Iwasaki,⁵¹ Y. Iwasaki,¹⁰ C. Jacoby,²² N. J. Joshi,⁴⁷
M. Kaga,²⁶ D. H. Kah,²¹ H. Kaji,²⁶ H. Kakuno,⁵¹ J. H. Kang,⁵⁷ P. Kapusta,³¹ S. U. Kataoka,²⁷
N. Katayama,¹⁰ H. Kawai,² T. Kawasaki,³³ A. Kibayashi,¹⁰ H. Kichimi,¹⁰ H. J. Kim,²¹
H. O. Kim,²¹ J. H. Kim,⁴⁵ S. K. Kim,⁴³ Y. I. Kim,²¹ Y. J. Kim,⁶ K. Kinoshita,³ S. Korpar,^{24,17}
Y. Kozakai,²⁶ P. Križan,^{23,17} P. Krokovny,¹⁰ R. Kumar,³⁷ E. Kurihara,² Y. Kuroki,³⁶
A. Kuzmin,¹ Y.-J. Kwon,⁵⁷ S.-H. Kyeong,⁵⁷ J. S. Lange,⁵ G. Leder,¹⁴ J. Lee,⁴³ J. S. Lee,⁴⁵
M. J. Lee,⁴³ S. E. Lee,⁴³ T. Lesiak,³¹ J. Li,⁹ A. Limosani,²⁵ S.-W. Lin,³⁰ C. Liu,⁴² Y. Liu,⁶
D. Liventsev,¹⁶ J. MacNaughton,¹⁰ F. Mandl,¹⁴ D. Marlow,³⁹ T. Matsumura,²⁶ A. Matyja,³¹
S. McOnie,⁴⁶ T. Medvedeva,¹⁶ Y. Mikami,⁵⁰ K. Miyabayashi,²⁷ H. Miyata,³³ Y. Miyazaki,²⁶
R. Mizuk,¹⁶ G. R. Moloney,²⁵ T. Mori,²⁶ T. Nagamine,⁵⁰ Y. Nagasaka,¹¹ Y. Nakahama,⁵¹
I. Nakamura,¹⁰ E. Nakano,³⁵ M. Nakao,¹⁰ H. Nakayama,⁵¹ H. Nakazawa,²⁸ Z. Natkaniec,³¹
K. Neichi,⁴⁹ S. Nishida,¹⁰ K. Nishimura,⁹ Y. Nishio,²⁶ I. Nishizawa,⁵³ O. Nitoh,⁵⁴ S. Noguchi,²⁷
T. Nozaki,¹⁰ A. Ogawa,⁴⁰ S. Ogawa,⁴⁸ T. Ohshima,²⁶ S. Okuno,¹⁸ S. L. Olsen,^{9,13} S. Ono,⁵²
W. Ostrowicz,³¹ H. Ozaki,¹⁰ P. Pakhlov,¹⁶ G. Pakhlova,¹⁶ H. Palka,³¹ C. W. Park,⁴⁵ H. Park,²¹
H. K. Park,²¹ K. S. Park,⁴⁵ N. Parslow,⁴⁶ L. S. Peak,⁴⁶ M. Pernicka,¹⁴ R. Pestotnik,¹⁷ M. Peters,⁹
L. E. Piilonen,⁵⁶ A. Poluektov,¹ J. Rorie,⁹ M. Rozanska,³¹ H. Sahoo,⁹ Y. Sakai,¹⁰ N. Sasao,²⁰
K. Sayeed,³ T. Schietinger,²² O. Schneider,²² P. Schönmeier,⁵⁰ J. Schümann,¹⁰ C. Schwanda,¹⁴
A. J. Schwartz,³ R. Seidl,^{12,40} A. Sekiya,²⁷ K. Senyo,²⁶ M. E. Sevier,²⁵ L. Shang,¹³ M. Shapkin,¹⁵
V. Shebalin,¹ C. P. Shen,⁹ H. Shibuya,⁴⁸ S. Shinomiya,³⁶ J.-G. Shiu,³⁰ B. Shwartz,¹ V. Sidorov,¹
J. B. Singh,³⁷ A. Sokolov,¹⁵ A. Somov,³ S. Stanič,³⁴ M. Starič,¹⁷ J. Stypula,³¹ A. Sugiyama,⁴¹
K. Sumisawa,¹⁰ T. Sumiyoshi,⁵³ S. Suzuki,⁴¹ S. Y. Suzuki,¹⁰ O. Tajima,¹⁰ F. Takasaki,¹⁰
K. Tamai,¹⁰ N. Tamura,³³ M. Tanaka,¹⁰ N. Taniguchi,²⁰ G. N. Taylor,²⁵ Y. Teramoto,³⁵
I. Tikhomirov,¹⁶ K. Trabelsi,¹⁰ Y. F. Tse,²⁵ T. Tsuboyama,¹⁰ Y. Uchida,⁶ S. Uehara,¹⁰
Y. Ueki,⁵³ K. Ueno,³⁰ T. Uglov,¹⁶ Y. Unno,⁸ S. Uno,¹⁰ P. Urquijo,²⁵ Y. Ushiroda,¹⁰ Y. Usov,¹
Y. Usuki,²⁶ G. Varner,⁹ K. E. Varvell,⁴⁶ K. Vervink,²² S. Villa,²² A. Vinokurova,¹ C. C. Wang,³⁰
C. H. Wang,²⁹ J. Wang,³⁸ M.-Z. Wang,³⁰ P. Wang,¹³ X. L. Wang,¹³ M. Watanabe,³³
Y. Watanabe,¹⁸ R. Wedd,²⁵ J.-T. Wei,³⁰ J. Wicht,¹⁰ L. Widhalm,¹⁴ J. Wiechczynski,³¹
E. Won,¹⁹ B. D. Yabsley,⁴⁶ A. Yamaguchi,⁵⁰ H. Yamamoto,⁵⁰ M. Yamaoka,²⁶ Y. Yamashita,³²
M. Yamauchi,¹⁰ C. Z. Yuan,¹³ Y. Yusa,⁵⁶ C. C. Zhang,¹³ L. M. Zhang,⁴² Z. P. Zhang,⁴²
V. Zhilich,¹ V. Zhulanov,¹ T. Zivko,¹⁷ A. Zupanc,¹⁷ N. Zwahlen,²² and O. Zyukova¹

arXiv:0808.1059v1 [hep-ex] 7 Aug 2008

(The Belle Collaboration)

- ¹*Budker Institute of Nuclear Physics, Novosibirsk*
- ²*Chiba University, Chiba*
- ³*University of Cincinnati, Cincinnati, Ohio 45221*
- ⁴*Department of Physics, Fu Jen Catholic University, Taipei*
- ⁵*Justus-Liebig-Universität Gießen, Gießen*
- ⁶*The Graduate University for Advanced Studies, Hayama*
- ⁷*Gyeongsang National University, Chinju*
- ⁸*Hanyang University, Seoul*
- ⁹*University of Hawaii, Honolulu, Hawaii 96822*
- ¹⁰*High Energy Accelerator Research Organization (KEK), Tsukuba*
- ¹¹*Hiroshima Institute of Technology, Hiroshima*
- ¹²*University of Illinois at Urbana-Champaign, Urbana, Illinois 61801*
- ¹³*Institute of High Energy Physics, Chinese Academy of Sciences, Beijing*
- ¹⁴*Institute of High Energy Physics, Vienna*
- ¹⁵*Institute of High Energy Physics, Protvino*
- ¹⁶*Institute for Theoretical and Experimental Physics, Moscow*
- ¹⁷*J. Stefan Institute, Ljubljana*
- ¹⁸*Kanagawa University, Yokohama*
- ¹⁹*Korea University, Seoul*
- ²⁰*Kyoto University, Kyoto*
- ²¹*Kyungpook National University, Taegu*
- ²²*École Polytechnique Fédérale de Lausanne (EPFL), Lausanne*
- ²³*Faculty of Mathematics and Physics, University of Ljubljana, Ljubljana*
- ²⁴*University of Maribor, Maribor*
- ²⁵*University of Melbourne, School of Physics, Victoria 3010*
- ²⁶*Nagoya University, Nagoya*
- ²⁷*Nara Women's University, Nara*
- ²⁸*National Central University, Chung-li*
- ²⁹*National United University, Miao Li*
- ³⁰*Department of Physics, National Taiwan University, Taipei*
- ³¹*H. Niewodniczanski Institute of Nuclear Physics, Krakow*
- ³²*Nippon Dental University, Niigata*
- ³³*Niigata University, Niigata*
- ³⁴*University of Nova Gorica, Nova Gorica*
- ³⁵*Osaka City University, Osaka*
- ³⁶*Osaka University, Osaka*
- ³⁷*Panjab University, Chandigarh*
- ³⁸*Peking University, Beijing*
- ³⁹*Princeton University, Princeton, New Jersey 08544*
- ⁴⁰*RIKEN BNL Research Center, Upton, New York 11973*
- ⁴¹*Saga University, Saga*
- ⁴²*University of Science and Technology of China, Hefei*
- ⁴³*Seoul National University, Seoul*
- ⁴⁴*Shinshu University, Nagano*
- ⁴⁵*Sungkyunkwan University, Suwon*
- ⁴⁶*University of Sydney, Sydney, New South Wales*
- ⁴⁷*Tata Institute of Fundamental Research, Mumbai*

⁴⁸*Toho University, Funabashi*

⁴⁹*Tohoku Gakuin University, Tagajo*

⁵⁰*Tohoku University, Sendai*

⁵¹*Department of Physics, University of Tokyo, Tokyo*

⁵²*Tokyo Institute of Technology, Tokyo*

⁵³*Tokyo Metropolitan University, Tokyo*

⁵⁴*Tokyo University of Agriculture and Technology, Tokyo*

⁵⁵*Toyama National College of Maritime Technology, Toyama*

⁵⁶*Virginia Polytechnic Institute and State University, Blacksburg, Virginia 24061*

⁵⁷*Yonsei University, Seoul*

Abstract

Using the high statistics τ data sample recorded in the Belle experiment at KEKB, we have greatly improved the precision of the branching fraction $\mathcal{B}(\tau^- \rightarrow K^{*0}(892)K^- \nu_\tau) = (1.56 \pm 0.02 \pm 0.09) \times 10^{-3}$, while the mass and width of the $K^{*0}(892)$ meson are measured to be $(895.10 \pm 0.27 \pm 0.31)$ MeV/ c^2 and $(47.23 \pm 0.49 \pm 0.79)$ MeV/ c^2 , respectively, with better accuracy than the PDG world average values. The first measurement of the decay $\tau^- \rightarrow K^{*0}(892)K^- \pi^0 \nu_\tau$ is also reported with a branching fraction of $\mathcal{B}(\tau^- \rightarrow K^{*0}(892)K^- \pi^0 \nu_\tau) = (2.39 \pm 0.46 \pm 0.26) \times 10^{-5}$.

INTRODUCTION

In addition to high statistics samples of B mesons, B factories also provide large number of τ -leptons, which can be used for high precision measurements. We report here a study of the decay $\tau^- \rightarrow K^{*0}(892)K^- \nu_\tau$, in which its branching fraction, as well as the mass, $M_{K^{*0}}$, and width, $\Gamma_{K^{*0}}$, of the $K^{*0}(892)$ resonance¹ are determined.

The measurement was performed with the Belle detector at the KEKB asymmetric-energy e^+e^- (3.5 on 8 GeV) collider [1], using the reaction $e^+e^- \rightarrow \tau^+\tau^-$. In this analysis we use a 544.9 fb^{-1} data sample recorded on and near the $\Upsilon(4S)$ resonance, corresponding to 5.0×10^8 produced $\tau^+\tau^-$ pairs.

The Belle detector is a large-solid-angle magnetic spectrometer that consists of a silicon vertex detector (SVD), a 50-layer central drift chamber (CDC), an array of aerogel threshold Cherenkov counters (ACC), a barrel-like arrangement of time-of-flight scintillation counters (TOF), and an electromagnetic calorimeter (ECL) comprised of CsI(Tl) crystals located inside a superconducting solenoid coil that provides a 1.5 T magnetic field. An

iron flux-return located outside the coil is instrumented to detect K_L^0 mesons and to identify muons (KLM). The detector is described in detail elsewhere [2].

Particle identification (PID) plays an important rôle in this experiment and is based on a likelihood ratio $\mathcal{P}_x \equiv L_x / \sum_y L_y$ for a charged particle $x = \mu, e, K, \text{ or } \pi$, where the sum runs over the relevant particles. L_x is a likelihood based on the energy deposit and shower shape in the ECL, the momentum and dE/dX measured by the CDC, the particle range in the KLM, the light yield in the ACC, and particle's time-of-flight from the TOF.

EVENT SELECTION

We look for $\tau^- \rightarrow K^{*0}(892)K^- \nu_\tau$ candidates with the following signature:

$$\begin{aligned} \tau_{\text{signal}}^- &\rightarrow K^{*0}(892) + K^- + (\text{missing}) \\ &\hookrightarrow K^+ \pi^- \\ \tau_{\text{tag}}^+ &\rightarrow (\mu/e)^+ + n(\leq 1)\gamma + (\text{missing}). \end{aligned}$$

An event should contain 4 charged tracks with zero net-charge. The following basic criteria are imposed; the total energy of the tracks and photons in the center-of-mass (CM) frame should be less than 11 GeV; the missing momentum should be greater than 0.1 GeV/ c and

¹ We hereafter simply denote the $K^{*0}(892)$ meson as K^{*0} .

lie within the detector acceptance $-0.866 < \cos \theta < 0.956$. The event is subdivided into two hemispheres according to the thrust axis in the CM frame, the signal and tag sides. The signal side contains three prongs and no additional photons while the one-prong side may include one extra photon.

On the tag side, $\mathcal{P}_{\mu/e} > 0.1$ is required for the track, while on the signal side the requirements $\mathcal{P}_K > 0.8$ ($\mathcal{P}_\pi > 0.8$) with $\mathcal{P}_e < 0.9$ are imposed for both kaons with opposite charges (for the K^{*0} daughter pion) within $\cos \theta > -0.6$. Here θ is the polar angle with respect to the z axis, which is anti-parallel to the e^+ beam direction. The three signal candidate tracks must have charge assignments that satisfy strangeness conservation i.e. $\tau^\mp \rightarrow K^{*0}(K^\pm \pi^\mp)K^\mp$.

In order to reduce $q\bar{q}$ background, the momenta of the K^{*0} and $K^{*0}K^-$ system are required to satisfy the requirements $p_{K^{*0}}^{\text{CM}} > 1.5$ GeV/c and $p_{K^{*0}K}^{\text{CM}} > 3.5$ GeV/c, respectively; the opening angles between the K^{*0} and K^- and between the thrust axis and missing momentum should satisfy the requirements $\cos \theta_{K^{*0}-K}^{\text{CM}} > 0.92$ and $\cos \theta_{\text{thrust-miss}}^{\text{CM}} < -0.6$, respectively; the invariant masses of the particles on both the tag and signal sides should be in the ranges $M_{\text{tag}} < 1.8$ GeV/c² ($\simeq m_\tau$) and

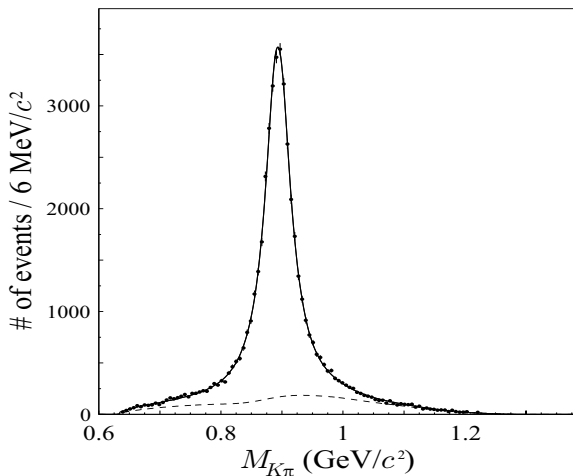


Fig. 1: $K^+\pi^-$ mass distribution after the selection. Data are indicated by points with error bars. The solid curve is the best fit result and the dashed curve is the incoherent BG $N^{\text{incoh}}(M_{K\pi})$, see the text for details.

$M_{\text{signal}} < 1.8$ GeV/c².

After applying all the selections, 5.1×10^4 events remain, and yield the $K^+\pi^-$ mass ($M_{K\pi}$) distribution, shown in Fig. 1. A clear K^{*0} peak is seen.

The detection efficiency (ϵ) for $\tau^- \rightarrow K^{*0}K^-\nu_\tau$ is evaluated using the KKMC/PYTHIA Monte Carlo (MC) program [3], where the V-A interaction is assumed for the weak vertices and all the final state particles are produced according to pure phase space. For $K^{*0} \rightarrow K^+\pi^-$, a spin-dependent Breit-Wigner (BW) function is used. The resulting efficiency, ϵ , is 2.15% which includes the branching fraction $\mathcal{B}(K^{*0} \rightarrow K^+\pi^-) = 2/3$ as well as the tagging efficiency.

BACKGROUNDS

The dominant background (BG) is from other generic decay modes of τ lepton pairs. The largest component, composing $\sim 80\%$ of the BG, arises from $\tau^- \rightarrow \pi^+\pi^-K^-n\pi^0\nu_\tau$ and $\tau^- \rightarrow \pi^+\pi^-\pi^-n\pi^0\nu_\tau$ with $n = 0$ and 1, through $\pi^+ \rightarrow K^+$ misidentification, and an undetected π^0 . We prepare such enriched BG samples from data by replacing the K^+ selection criteria $\mathcal{P}_K > 0.8$ by $\mathcal{P}_K < 0.2$ ($K^+ \rightarrow \pi^+$), and estimate the contamination in the $K^{*0}K^-\nu_\tau$ samples, taking into account the PID fake rate. This estimate has a 1.1% systematic uncertainty, mostly due to errors in the PID fake rate.

Another $\sim 20\%$ of BG is attributed to $\tau^- \rightarrow \phi K^-\nu_\tau$, $K^+\pi^-K^-\pi^0\nu_\tau$ (excluding K^{*0}), $\phi\pi^-\nu_\tau$, and $K^+\pi^-K^-\nu_\tau$ (ex. K^{*0}), and is estimated by MC simulation. The first and second background components arise from misPID ($K^- \rightarrow \pi^-$) and missing π^0 detection, respectively, at rates of $(1.4 \pm 0.2)\%$ and $(2.1 \pm 0.7)\%$. Their $M_{K\pi}$ spectra are evaluated by MC, based on their branching fractions, reported in Refs. [4] and [5], with uncertainties of 0.07% and 0.6% of the K^{*0} yields.

The third background component has the same final state, $K^+\pi^-K^-\nu_\tau$, as that of $K^{*0}K^-\nu_\tau$, and its $M_{K\pi}$ spectrum

($N^{\phi\pi^- \nu}(M_{K\pi})$) is obtained in [6]. The fourth BG is the non-resonant (NR) component and can interfere with the signal. Details are discussed in the next section.

On the other hand, K^{*0} -resonant BG comes from as yet unmeasured $\tau^- \rightarrow K^{*0}K^-\pi^0\nu_\tau$ decay and $q\bar{q}$ processes. In order to measure $\mathcal{B}(\tau^- \rightarrow K^{*0}K^-\pi^0\nu_\tau)$, we apply the same criteria as for the $K^{*0}K^-\nu_\tau$ selection, but with additional requirements of $n_\gamma = 2$ and effective mass ($M_{\gamma\gamma}$) in the range, $0.1178 \text{ GeV}/c^2 < M_{\gamma\gamma} < 0.1502 \text{ GeV}/c^2$. Figure 2 shows the resulting $M_{K\pi}$ distribution, where the K^{*0} peak includes two contributions: one is the $K^{*0}K^-\pi^0\nu_\tau$ signal, and the other comes from $K^{*0}K^-\nu_\tau$ events with a π^0 formed by spurious photons, caused by a splitoff of a hadronic shower in the ECL calorimeter. The latter contribution is calculated by MC, using $\mathcal{B}(\tau^- \rightarrow K^{*0}K^-\nu_\tau)$ from the PDG [5] and our result. The non- K^{*0} BG in Fig. 2 mostly arises from $\tau^+\tau^-$ pair processes, while the $q\bar{q}$ contribution is negligibly small. The $M_{K\pi}$ distribution is fitted with a K^{*0} BW function plus a non- K^{*0} BG represented by a Landau function, with four free parameters: the total number of $K^{*0}K^-\pi^0\nu_\tau$ events, and three parameters of the Landau function. The best fit yields the number of signal events as $N_{K^{*0}K^-\pi^0\nu} = 129.2 \pm 25.1$, with a detection efficiency $\epsilon = 0.54\%$, fixing the $K^{*0}K^-\nu_\tau$ peaking BG to $N_{K^{*0}K^-\nu} = 113.7 \pm 6.8$ events. As a result, we obtain the first measurement of the branching fraction,

$$\mathcal{B}(\tau^- \rightarrow K^{*0}K^-\pi^0\nu_\tau) = (2.39 \pm 0.46 \pm 0.26) \times 10^{-5}, \quad (1)$$

with a systematic uncertainty of 11.0%. Table II lists the sources of individual uncertainties. The largest contribution, 9.0%, arises from an uncertainty on the peaking BG estimate, especially, on $\tau^- \rightarrow K^{*0}K^-\nu_\tau$. This $K^{*0}K^-\pi^0\nu_\tau$ contamination in the $K^{*0}K^-\nu_\tau$ signal in the $M_{K\pi}$ distribution is only 0.4%.

The other possible K^{*0} -resonant BG, the $q\bar{q}$ contribution, mostly from uds , is examined in a comparison between data and MC, by applying $q\bar{q}$ enriching selection criteria. The estimated contribution in the K^{*0} mass region is

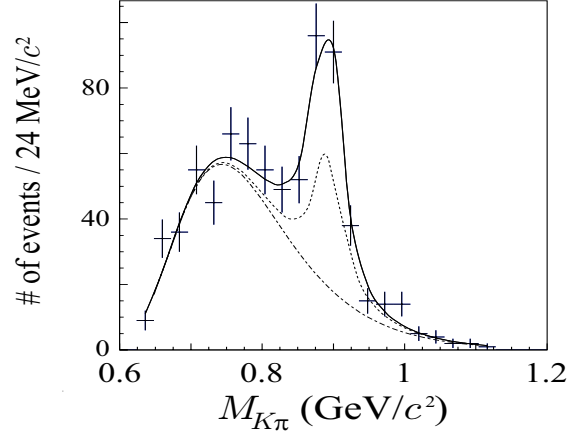


Fig. 2: $K^+\pi^-$ mass distribution for $K^{*0}K^-\pi^0\nu_\tau$ candidates. Data are plotted by crosses, and the best-fit result is indicated by the solid curve, the $K^{*0}K^-\nu_\tau$ contamination and the non- K^{*0} BG are shown by the dotted curve and dash-dotted one, respectively. See the text for details.

46 ± 17 events: It gives an uncertainty of only 0.14% to the estimation of the signal events for the $K^{*0}K^-\nu_\tau$ analysis.

$\mathcal{B}(\tau^- \rightarrow K^{*0}K^-\nu_\tau)$

The $M_{K\pi}$ distribution in Fig. 1 is fitted with the following formula:

$$N(M_{K\pi}) = \left| \alpha A_{BW}(M_{K\pi}) + \beta A_{NR}(M_{K\pi}) e^{i\phi} \right|^2 + N^{\phi\pi^- \nu}(M_{K\pi}) + N^{\text{incoh}}(M_{K\pi}) \quad (2)$$

where $A_{BW}(M_{K\pi})$ is the Breit-Wigner (BW) function for the decay of a $J^P = 1^- \rightarrow 0^-0^-$ state, expressed as

$$A_{BW}(M_{K\pi}) = \frac{M_0 \Gamma}{(M_0^2 - M_{K\pi}^2) - i M_0 \Gamma},$$

$$\Gamma(M_{K\pi}) = \left(\frac{q}{q_0} \right)^3 \left(\frac{M_0}{M_{K\pi}} \right) \frac{D_L(q_0 r)}{D_L(q r)} \Gamma_0. \quad (3)$$

M_0 and Γ_0 are the $M_{K^{*0}}$ and $\Gamma_{K^{*0}}$, respectively. q is the momentum in the $K^+\pi^-$ center of mass, and $D_L(qr) = 1/(1 + r^2 q^2)$ is the barrier factor with the so-called damping factor r . Since the damping factors for $K^{*0}(892) \rightarrow K^+\pi^-$ decay were obtained by LASS [7] in the $K^-p \rightarrow K\pi n$ reaction, $r = 3.4 \pm 0.6 \pm 0.3 (\text{GeV}/c)^{-1}$, and by FOCUS [8]

Table I: Results of fits over the mass region of $0.645 - 1.147$ (GeV/c^2). 'standard' means the fit with five free parameters (α , β , M_{K^*0} , Γ_{K^*0} and ϕ) with $r = 3.53$, and with $r = 0$. The interference between A_{BW} and A_{NR} is excluded in the 'no interference' case, and then ϕ is removed from the fit. In the rightmost column, A_{NR} is omitted in the fit. To obtain branching fractions, we use detection efficiencies, as $\epsilon_{K^*K} = (2.15 \pm 0.01)\%$ and $\epsilon_{KK\pi} = (2.60 \pm 0.01)\%$, determined from MC simulations based on pure hadronic phase space with a $V - A$ weak interaction. In $\mathcal{B}(\tau^- \rightarrow K^*0 K^- \nu_\tau)$, $\mathcal{B}(K^*0 \rightarrow K^+ \pi^-) = 2/3$ is included.

	standard		no interference	no A_{NR}
	$r = 3.53$	$r = 0.0$	$r = 3.53$	$r = 3.53$
M_{K^*0} (MeV/c^2)	895.25 ± 0.27	896.58 ± 0.28	896.72 ± 0.19	896.85 ± 0.19
Γ_{K^*0} (MeV/c^2)	47.70 ± 0.49	48.19 ± 0.51	47.45 ± 0.48	49.21 ± 0.46
ϕ ($^\circ$)	63.46 ± 2.05	37.98 ± 2.90	—	—
$\mathcal{B}(K^*0 K^- \nu)$ ($\times 10^{-3}$)	1.56 ± 0.02	1.55 ± 0.02	1.80 ± 0.01	1.84 ± 0.01
$\mathcal{B}(K^+ \pi^- K^- \nu)$ ($\times 10^{-5}$)	5.76 ± 0.59	4.62 ± 0.53	4.82 ± 0.54	—
χ^2/ndf	83.29/80	84.64/80	146.3/81	226.2/82

in $D^+ \rightarrow K^- \pi^+ \mu^+ \nu$ decay, $r = 3.96 \pm 0.54_{-0.90}^{+1.31}$ (GeV/c) $^{-1}$, we take the average of these two values, $r = 3.53 \pm 0.59$ (GeV/c) $^{-1}$ in the fits. The term $A_{NR}(M_{K\pi})$ is the non-resonant $\tau^- \rightarrow K^+ \pi^- K^- \nu_\tau$ scalar amplitude, and can be expressed as

$$A_{NR} = \left(\frac{M_{K\pi}}{q} \right) \sin \delta_{LASS} e^{i\delta_{LASS}} \quad (4)$$

where the phase-shift of δ_{LASS} is parametrized as

$$\cot \delta_{LASS} = \frac{1}{aq} + \frac{bq}{2} \quad (5)$$

following the LASS [7] and FOCUS [8] analyses with $a = 4.03 \pm 1.72 \pm 0.06$ (GeV) $^{-1}$ and $b = 1.29 \pm 0.63 \pm 0.67$ (GeV) $^{-1}$, obtained by LASS. The phase δ_{LASS} has a weak q -dependence and is $\simeq 45^\circ$ in our momentum range. Since the final hadronic system contains an additional K^- , final state interactions are possible between K^*0 and non-resonant $K^+ \pi^-$ systems and K^- , and a relative phase between the A_{BW} and A_{NR} amplitudes is introduced in the formula. Here, $N^{\phi\pi^- \nu}(M_{K\pi})$ is the contribution from $\phi\pi^- \nu_\tau$, and $N^{\text{incoh}}(M_{K\pi})$ is the sum of the incoherent continuum and peaking BG's discussed in the previous section. These correspond to 795 ± 65 and $10,073 \pm 994$ events, respectively. The free parameters in the χ^2 -fits are α , β , M_{K^*0} , Γ_{K^*0} , and ϕ .

The mass dependence of the resolution is taken into account in the fit. The resolution function can be approximated as a sum of three Gaussian functions with their relative fractions and standard deviations σ 's: about 52% with 1.7 MeV/c^2 , 38% with 3.4 MeV/c^2 and 10% with 9.2 MeV/c^2 at $M_{K\pi} \simeq 890$ MeV/c^2 ; σ 's vary by 3.7×10^{-3} , 5.6×10^{-3} and 3.3×10^{-3} per MeV/c^2 with $M_{K\pi}$, respectively; the third Gaussian is shifted to the higher mass side by $\simeq 0.13$ MeV/c^2 relative to the others.

The χ^2 -fits are performed in the mass range $M_{K\pi} = 0.645 - 1.147$ (GeV/c^2). The results of fits are listed in Table I, and the best fit is shown in Figs. 1 and 3. The branching fractions obtained are $\mathcal{B}(\tau^- \rightarrow K^*0 K^- \nu_\tau) = (1.56 \pm 0.02) \times 10^{-3}$ and $\mathcal{B}(\tau^- \rightarrow K^+ \pi^- K^- \nu_\tau)_{\text{non-resonant}} = (5.76 \pm 0.59) \times 10^{-5}$. The non-resonant $K^+ \pi^- K^- \nu_\tau$ contribution is $(5.58 \pm 0.57)\%$, which agrees well with the FOCUS result of $(5.30 \pm 0.74_{-0.96}^{+0.99})\%$.

Since $\phi + \delta_{LASS} \simeq 65^\circ + 45^\circ \simeq 110^\circ$, the interference term $2\alpha\beta A_{BW} A_{NR}^*$ has a $M_{K\pi}$ distribution similar to a BW shape, as seen in Fig. 3. The role of the damping factor in the $M_{K\pi}$ distribution in this reaction resembles that of ϕ in the interference term on the distribution. This can be seen in the $\phi = 0^\circ$ case, where the parameters resulting from the fit, except for ϕ , do not change much compared to the $r = 3.53$ case, while ϕ changes

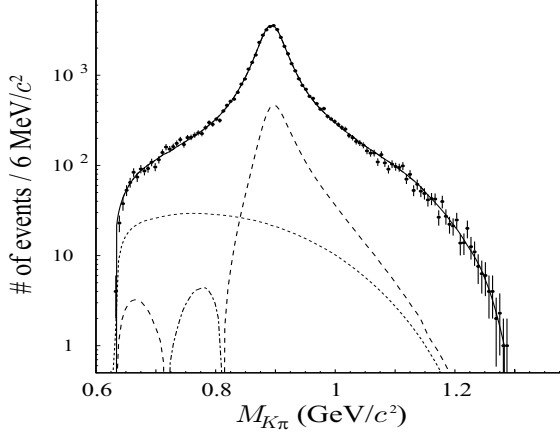


Fig. 3: Result of the best-fit, plotted with a logarithmic scale. The spectra of all terms, the interference term and the non-resonant term are plotted by the solid, dashed and dotted curves, respectively. The negative interference term is reversed and plotted by the dash-dotted curve. See Fig. 1 for the same plot, but with a linear scale.

from $(37.98 \pm 2.90)^\circ$ to $(63.46 \pm 2.05)^\circ$ with a χ^2 difference of $\Delta\chi^2 = 1.35$.

When the interference contribution is not taken into account, $\mathcal{B}(\tau^- \rightarrow K^{*0}K^- \nu_\tau)$ becomes 15% larger (see the fourth column in Table I); when the NR contribution is totally ignored, $\mathcal{B}(\tau^- \rightarrow K^{*0}K^- \nu_\tau)$ becomes 2.2% larger than in the case where the interference contribution is not taken into account (see the rightmost column in Table I).

The systematic uncertainties are listed in Table II. The total uncertainty is 5.5%, where the largest errors are attributed to the track finding efficiency, and PID's on the lepton and kaon, as 3.3%, 2.9% and 2.6%, respectively. The r parameter is varied by $\pm 1\sigma$ to evaluate its effect on the branching fractions: the resulting change is $\pm 0.3\%$ for $\mathcal{B}(\tau^- \rightarrow K^{*0}K^- \nu_\tau)$ and $\pm 1.6\%$ for $\mathcal{B}(\tau^- \rightarrow K^+\pi^-K^- \nu_\tau)$. These systematic uncertainties are much smaller than the statistical error of the fit.

Adding all systematic errors in quadrature, the branching fraction obtained is

$$\mathcal{B}(\tau^- \rightarrow K^{*0}K^- \nu_\tau) = (1.56 \pm 0.02 \pm 0.09) \times 10^{-3}. \quad (6)$$

The branching fraction of non-resonant

$\tau^- \rightarrow K^+\pi^-K^- \nu_\tau$ is also obtained,

$$\mathcal{B}(\tau^- \rightarrow K^+\pi^-K^- \nu_\tau)_{\text{non-resonant}} = (5.76 \pm 0.59 \pm 2.04) \times 10^{-5}. \quad (7)$$

This is the first measurement of non-resonant $\tau^- \rightarrow K^+\pi^-K^- \nu_\tau$ decay, where the large systematic error mostly comes from the uncertainty in estimating the $\pi^+\pi^-\pi^- \nu_\tau$ BG contamination through mis-PID.

$M_{K^{*0}}$ AND $\Gamma_{K^{*0}}$

The absolute mass scale for the Belle detector is confirmed by reconstructing the K_S and ϕ masses through their $\pi^-\pi^+$ and K^-K^+ decay modes, respectively, and comparing them to their world average values. Such studies provide mass differences from the PDG values [5] of -0.045 ± 0.027 MeV/ c^2 and -0.14 ± 0.20 MeV/ c^2 for M_{K_S} and M_ϕ , respectively, or from the most precise measurements [9] and [10], -0.022 ± 0.035 MeV/ c^2 and -0.12 ± 0.20 MeV/ c^2 . Therefore, no correction is applied to the absolute mass scale.

On the other hand, MC simulation results in shifts of $\Delta M_{K^{*0}} = 0.15 \pm 0.04$ MeV/ c^2 and $\Delta \Gamma_{K^{*0}} = 0.47 \pm 0.22$ MeV/ c^2 , due to the effects of detection efficiency and event selections, and therefore we correct the raw $M_{K^{*0}}$ and $\Gamma_{K^{*0}}$ values by these amounts, respectively.

Table II: Systematic errors for $\mathcal{B}(\tau^- \rightarrow K^{*0}K^- \nu_\tau)$ (left column) and $\mathcal{B}(\tau^- \rightarrow K^{*0}K^- \pi^0 \nu_\tau)$ (right column) in %.

	$K^{*0}K^- \nu$	$K^{*0}K^- \pi^0 \nu$
Luminosity	1.4	1.4
$\sigma(e^+e^- \rightarrow \tau\tau)$	0.3	0.3
Tracking efficiency	3.3	3.3
Trigger efficiency	0.7	0.1
Lepton-ID	2.9	2.9
Kaon-ID/fake	2.6	3.8
MC statistics	0.3	0.5
π^0 efficiency	–	1.7
BG estimate	1.3	9.0
Total	5.5	11.0

Table III: Comparison of our results with other experiments

	$M_{K^{*0}}(892)$ (MeV/c ²)	$\Gamma_{K^{*0}}(892)$ (MeV/c ²)
Belle	$895.10 \pm 0.27 \pm 0.31$	$47.23 \pm 0.49 \pm 0.79$
PDG [5]	896.00 ± 0.25	50.3 ± 0.6
FOCUS [8]	$895.41 \pm 0.32 \pm_{0.43}^{0.35}$	$47.79 \pm 0.86 \pm_{1.06}^{1.32}$
LASS [7]	$895.9 \pm 0.5 \pm 0.2$	$50.8 \pm 0.8 \pm 0.9$
	$M_{K^{*\pm}}(892)$ (MeV/c ²)	$\Gamma_{K^{*\pm}}(892)$ (MeV/c ²)
Belle [11]	$895.47 \pm 0.20 \pm 0.74$	$46.2 \pm 0.6 \pm 1.2$
PDG [5]	891.66 ± 0.26	50.8 ± 0.9

To evaluate uncertainties in the BG estimates on $M_{K^{*0}}$ and $\Gamma_{K^{*0}}$, we vary the mis-PID probabilities by $\pm 1\sigma$ in the fit. The resulting variation is $\delta M_{K^{*0}} = \pm 0.23 \text{ MeV}/c^2$ and $\delta \Gamma_{K^{*0}} = \pm 0.75 \text{ MeV}/c^2$. The uncertainty in r is included by varying it by $\pm 1\sigma$ in the fit, which gives changes of $M_{K^{*0}} = \pm 0.22 \text{ MeV}/c^2$ and $\Gamma_{K^{*0}} = \pm 0.09 \text{ MeV}/c^2$.

Including the above errors in quadrature, the mass and width are

$$M_{K^{*0}} = 895.10 \pm 0.27 \pm 0.31 \text{ (MeV}/c^2), \quad (8)$$

$$\Gamma_{K^{*0}} = 47.23 \pm 0.49 \pm 0.79 \text{ (MeV}/c^2), \quad (9)$$

where the first and second errors are statistical and systematic ones, respectively.

CONCLUSIONS

With the use of high-statistics data samples of 544.9 fb^{-1} , collected in the Belle experiment, we have measured $\mathcal{B}(\tau^- \rightarrow K^{*0} K^- \nu_\tau)$ with the highest precision so far attained, and obtained the first measurements of $\mathcal{B}(\tau^- \rightarrow K^{*0} K^- \pi^0 \nu_\tau)$ and $\mathcal{B}(\tau^- \rightarrow K^+ \pi^- K^- \nu_\tau)_{\text{non-resonant}}$, respectively.

The K^{*0} mass and width are also measured, respectively, with better or same accuracy than those of the PDG world average values, or the most precise previous experiments, as listed in Table III.

Figure 4 compares various measurements: our results differ from the PDG world average values, but are quite consistent with the results of the FOCUS experiment for $M_{K^{*0}}$ and $\Gamma_{K^{*0}}$. The difference between our measurement of $\mathcal{B}(\tau^- \rightarrow K^{*0} K^- \nu_\tau)$ and other results

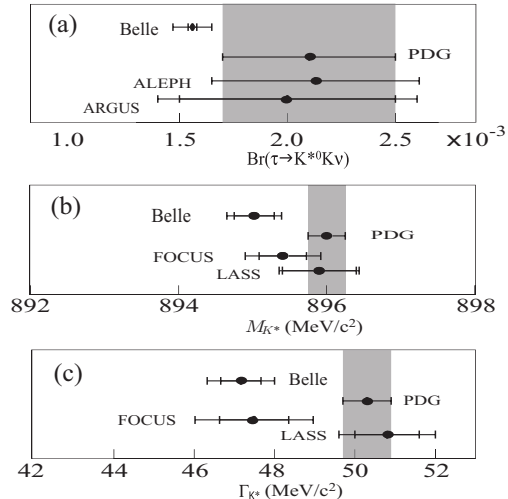


Fig. 4: Comparison of various measurements: (a) $\mathcal{B}(\tau^- \rightarrow K^{*0} K^- \nu_\tau)$, (b) $M_{K^{*0}}$ and (c) $\Gamma_{K^{*0}}$. In (a), the PDG value is obtained from ARGUS [12] and ALEPH [13]. In (b) and (c), FOCUS and LASS results are included in the PDG value.

may be due to the inclusion of the interference effect between the decays that have the same final state $K^+ \pi^- K^- \nu_\tau$.

Acknowledgements

We thank the KEKB group for the excellent operation of the accelerator, the KEK cryogenics group for the efficient operation of the solenoid, and the KEK computer group and the National Institute of Informatics for valuable computing and SINET3 network support. We acknowledge support from the Ministry of Education, Culture, Sports, Science, and Technology of Japan and the Japan Society for the Promotion of Science; the Australian

Research Council and the Australian Department of Education, Science and Training; the National Natural Science Foundation of China under contract No. 10575109 and 10775142; the Department of Science and Technology of India; the BK21 program of the Ministry of Education of Korea, the CHEP SRC program and Basic Research program (grant No. R01-2005-000-10089-0) of the Korea Science and Engineering Foundation, and the Pure Basic Research Group program of the Korea Research Foundation; the Polish State Committee for Scientific Research; the Ministry of Education and Science of the Russian Federation and the Russian Federal Agency for Atomic Energy; the Slovenian Research Agency; the Swiss National Science Foundation; the National Science Council and the Ministry of Education of Taiwan; and the U.S. Department of Energy.

[1] S. Kurokawa, E. Kikutani, Nucl. Instrum. Methods A **499** (2003) 1.
 [2] A. Abashian *et al.* (Belle Collaboration),

Nucl. Instr. Meth. A **479** (2002) 117.
 [3] S. Jadach, B.F.L. Ward, Z. Was, Comp. Phys. Commun. **130** (2000) 260.
 [4] K. Inami *et al.* (Belle Collaboration), Phys. Lett. B **643** (2006) 5. $\mathcal{B}(\tau^- \rightarrow \phi K^- \nu_\tau) = (4.05 \pm 0.25 \pm 0.26) \times 10^{-5}$ and $\mathcal{B}(\tau^- \rightarrow \phi \pi^- \nu_\tau) = (6.05 \pm 0.71) \times 10^{-5}$ are used, while the latter is not their final value.
 [5] W.-M. Yao *et al.* (Particle Data Group), J. Phys. G **33** (2006) 1.
 [6] K. Hayasaka *et al.* (Belle Collaboration), to be published. See Fig. 2 for the $M_{K\pi}$ spectrum of the $\phi\pi$ contribution.
 [7] D. Aston *et al.* (LASS Collaboration), Nucl. Phys. B **296** (1988) 493.
 [8] J.M. Link *et al.* (FOCUS Collaboration), Phys. Lett. B **621** (2005) 72.
 [9] A. Lai *et al.* (NA48 Collaboration), Phys. Lett. B **533** (2002) 196.
 [10] R.R. Akhmetshin *et al.* (CMD-2 Collaboration), Phys. Lett. B **578** (2004) 285.
 [11] D. Epifanov *et al.* (Belle Collaboration), Phys. Lett. B **654** (2007) 65.
 [12] H. Albrecht *et al.* (ARGUS Collaboration), Z. Phys. C **68** (1995) 215.
 [13] R. Barate *et al.* (ALEPH Collaboration), Eur. Phys. J. C **1** (1998) 65.